Photon Cross Section Data in Absorbed Dose Calculations

J S Eakins

ABSTRACT

Air kerma data and the relative response of the new HPA TLD are calculated for Narrow Series X-ray distribution and ^{137}Cs photon sources using the general purpose Monte Carlo code MCNP5, and the results are compared to those obtained using its predecessor, MCNP4c2. It is found that the results differ at low energies (< 0.1 MeV) by up to ~10 %. This disparity is mainly ascribed to differences in the default photon interaction data used by the two codes, and derives ultimately from the influence on absorbed dose of the recent updates to the photoelectric effect cross sections. The sources of these data are reviewed, and their differences explored. The cross sections used to derive the commonly-used mass attenuation and mass-energy absorption coefficients, as well as air kerma to personal dose equivalent conversion coefficients, are also discussed, and the implications of these considered.

Centre for Radiation, Chemical and Environmental Hazards
Radiation Protection Division
Chilton, Didcot, Oxfordshire OX11 0RQ

Approval: December 2008
Publication: January 2009
£13.00
ISBN 978-0-85951-632-7

CONTENTS

1 INTRODUCTION

The Health Protection Agency (HPA) has recently updated its personal dosimetry service for estimating exposures in mixed photon/electron fields. In particular, a new personal thermoluminescence dosemeter (TLD) has been designed, developed and subsequently issued [Eakins *et al*, 2007; Gilvin *et al*, 2007] that assesses both $H_p(10)$ and $H_\mathrm{p}(0.07)$, appropriate for the energy range from a few keV to a few MeV. The design process was primarily undertaken using the general purpose Monte Carlo code MCNP4c2 [Briesmeister, 2000], backed up by measurements and experimental type-testing.

Since completing the above work, the newer code MCNP5 [X5 Team, 2003] has become available to users at HPA; this is an updated version of its predecessor, MCNP4c2. Because research into the new TLD is considered on-going, not least due to continued interest in its performance in novel or unusual circumstances and fields that can only or best be assessed via Monte Carlo modelling, as well as for general benchmarking, an obvious question is therefore posed: how, if at all, does the version of MCNP employed affect the results obtained? Specifically, are the response characteristics that are calculated when MCNP5 is used the same as those that were obtained previously using MCNP4c2? Of course, this issue has wider implications, and is not just restricted to the particular case of TLD performance.

The current article seeks to address this matter, and is in many ways an extension of the earlier work [Eakins *et al*, 2007] that detailed the Monte Carlo design of the HPA TLD, where the MCNP4c2 versus MCNP5 issue could be mentioned only briefly. Specifically, both air kerma and some of the TLD response data presented previously are recalculated using MCNP5, and in this paper the ratios of the results from the two codes are provided. This comparison in turn necessitates a discussion of the cross section data utilized by MCNP4c2 and by MCNP5. For completeness, the cross section data employed to derive the routinely-used mass attenuation and mass-energy absorption coefficients are also discussed, in part to illustrate aspects of the development from MCNP4c2 to MCNP5, and in part because these represent a common alternative to Monte Carlo methods in the assessment of absorbed photon doses in radiological protection. Also considered are the cross section data used to determine the relevant conversion coefficients required to evaluate the dosemeter response.

2 TLD RESPONSE

The HPA TLD is a passive, two-element dosemeter incorporating Mg/Cu/P-doped lithium fluoride (^{7}LiF:Mg,Cu,P) detectors in a Harshaw *TLD-700H* 'card'; the card is located inside a holder with polypropylene (PP) walls 2 mm thick, which features a hole in front of the $H_\mathrm{p}(0.07)$ element and a cylinder of polytetrafluoroethylene (PTFE) 4.3 mm thick and 18 mm in diameter in front of the $H_\mathrm{p}(10)$ element. The technical specifications and performance of the TLD are described in detail elsewhere [Eakins *et al*, 2007; Gilvin *et al*, 2007]. The relative response, $R(\theta,E)$, of the TLD for a plane-parallel photon source of mean energy E, incident at an angle θ, is calculated using the kerma approximation with the photon-only transport mode of MCNP, and is defined relative to ^{137}Cs via Equation (1), where: $K(\theta,E)_M$ is the absorbed dose or, equivalently here, kerma per-source-particle in the detector of interest (i.e. the $H_p(10)$ element or the $H_p(0.07)$ element), estimated from an MCNP '*f6:p*' tally, for detector material M (i.e. LiF or air); $h(\theta,E)$ is the air kerma to personal dose equivalent conversion coefficient at that energy and angle, for the protection quantity of interest; and $\eta'(E)$ is the relative thermoluminescence efficiency of the TLD-700H lithium fluoride at source energy E, corresponding to the measured light output per calculated absorbed dose (and normalized to ^{137}Cs), and prior estimated [Eakins *et al*, 2007] by a method that involved rearranging Equation (1) and comparing earlier MCNP4c2 data with experimental results.

$$R(\theta,E)=\left[\frac{\left(K(\theta,E)_{LiF}\big/K(0,E)_{air}\right)}{\left(K(0,Cs)_{LiF}\big/K(0,Cs)_{air}\right)}\right]\times\frac{h(0,Cs)}{h(\theta,E)}\times\eta'(E) \qquad (1)$$

The MCNP *f6:p* track-length heating tally evaluates the photon energy deposition averaged over a region of interest, divided by the mass of that region; the estimate is achieved by considering the photon tracks through the volume, and the photon cross section and average heating per collision (incoherent, photoelectric and pair production) as a function of energy [Briesmeister, 2000; X5 Team, 2003]. Air kerma data, $K(\theta,E)_{air}$ ($\equiv K(0,E)_{air}$ here by definition), are calculated by repeating the simulations with all of the materials of the configuration redefined as air.

The sources of present interest are the 2.5 m Narrow Series distributions of X-ray radiation provided by Ankerhold [Ankerhold, 2000], corresponding to those produced by an experimental set-up similar to that prescribed by ISO 4037-1 [ISO, 1996], and a monoenergetic 0.662 MeV source representing caesium-137. The conversion coefficients used are taken either from [Ankerhold, 2000] Tables 4.19 and 4.20, or ISO 4037-3 [ISO, 1999] Tables 33 and A.6, as appropriate. The reasons behind these decisions, along with a description of the exact geometry used, are explored in the earlier work [Eakins *et al*, 2007]; what is important now is that the conversion coefficients, efficiency and input files used in the present simulations are identical to those used previously, with the only change being the version of MCNP employed. Thus as before, the dosemeter is positioned on the front of an ISO water-filled slab phantom, surrounded by vacuum; $\theta=0°$ represents the outward normal to the phantom front-face.

3 RESULTS

The performances of MCNP4c2 versus MCNP5 are perhaps best examined by ratio; for the TLD response comparison, such a method avoids the potential inclusion of any errors from either $h(\theta,E)$ or $\eta'(E)$. Figure 1 shows the ratio $A = [K(0,E)_{air,(5)}] \div [K(0,E)_{air,(4c2)}]$, where the bracketed subscript denotes the version of MCNP used in the calculation. The error bars in this and other figures in the present article represent one standard uncertainty on the result, corresponding only to the statistical uncertainties from the Monte Carlo calculations. As can be seen, at low energies (i.e. below ~100 keV) the MCNP5 calculated air kerma is higher than that calculated by MCNP4c2, with the discrepancy peaking at around 25 keV.

Figure 1 also shows the ratios $L_x = [K(0,E)_{\mathrm{LiF},(5)}] \div [K(0,E)_{\mathrm{LiF},(4c2)}]$, where x is 10 or 0.07 to denote that the kerma are tallied in the H_p(x) element. Apart from for the H_p(10) detector for the source with a mean energy of 16 keV, the MCNP5 low-energy result is again seen generally to be higher than the MCNP4c2 result, though the contrast is typically less pronounced than for air.

The differences in the absorbed dose results for air and LiF can contribute to differences in the calculations of relative response; on the other hand, for some energies (at 48 keV for the H_p(10) element, for example) the differences can also effectively cancel out. Figure 2 shows, for both the H_p(10) and the H_p(0.07) elements, the ratios $[R(0,E)_{(5)}] \div [R(0,E)_{(4c2)}]$, where the above use of bracketed subscripts has again been adopted. As before, discrepancies between the results from the two codes are most clearly exhibited at low energies.

4 PHOTON INTERACTION DATA

Of the many changes made during the development from MCNP4c2 to MCNP5, the one that can perhaps best explain the differences found in the above results concerns the updating of the photon cross sections used. To illustrate this issue, it is first instructive to consider a short review of the chronological ‘evolution’ over the last few decades regarding the cross section data employed both by MCNP and in determining the oft-used mass attenuation and mass-energy absorption coefficients. Specifically, for the elements (low / intermediate Z) and energy range (~keV to ~MeV) of interest:

a According to its manual [Briesmeister, 2000], MCNP4c2 uses Evaluated Nuclear Data File (ENDF) photon interaction cross sections taken from [Hubbell *et al*, 1975], along with [Everett *et al*, 1973] fluorescence data;

b [Hubbell, 1982] mass attenuation / energy absorption coefficients are calculated from [Hubbell *et al*, 1975] (and its erratum, [Hubbell *et al*, 1977]) and [Hubbell & Øverbø, 1979] incoherent and coherent scattering data, with atomic photoelectric effect data taken from [Scofield, 1973]. The [Scofield, 1973] renormalization factors are applied;

c [Hubbell & Seltzer, 1995] mass attenuation / energy absorption coefficients are calculated using [Scofield, 1973] photoelectric cross sections and [Hubbell *et al*, 1975] (and its erratum, [Hubbell *et al*, 1977]) and [Hubbell & Øverbø, 1979] incoherent/coherent data. The [Scofield, 1973] data are ‘un-renormalized’, as a comparison with measurements by [Saloman *et al*, 1988] shows these to be more accurate;

d MCNP5 uses the updated ENDF/B-VI.8 library by default, which is in turn based upon the EPDL97 library of [Cullen *et al*, 1997]. The EPDL97 cross sections incorporate [Saloman *et al*, 1988] and [Hubbell & Seltzer, 1995] photoionization data, with coherent/incoherent scattering data from [Hubbell *et al*, 1975] (and its erratum, [Hubbell *et al*, 1977]), [Hubbell & Øverbø, 1979] and [Hubbell, 1997], and the anomalous scattering factors of [Cullen, 1989].

Further additions and updates, such as to pair and triplet production cross sections, atomic and photoexcitation data, photonuclear effects, energy grid modifications, expansion of the data sets to include more elements, etc., also feature during the above evolution. Both MCNP4c2 and MCNP5 use the *e103* library by default for electron interaction cross section data, derived from the ITS3.0 code system [Halbleib *et al*, 1992].

It is, of course, the photoelectric cross section that dominates in the low energy regime where the greatest differences between the MCNP4c2 and MCNP5 results are found, as exhibited in Figures 1 and 2.

4.1 Monte Carlo Data

It is wondered whether the description given in the MCNP4c2 manual [Briesmeister, 2000] is perhaps misleading in its terminology. Instead, the author of this present article interprets that 'fluorescence' there probably also includes photoelectric interactions, whilst only actually the coherent and incoherent data are taken from [Hubbell *et al*, 1975]. Justification for this proposal is that [Hubbell *et al*, 1975] appears not to focus on photoelectric data, whereas [Everett *et al*, 1973] deals primarily with a revision of the work of [Cashwell *et al*, 1973] by improving the electron ejection and fluorescent photon emission subroutines for photoelectric-induced events in MCP, a code from which MCNP grew. Both Cashwell and Everett make use of the cross sections of [Storm & Israel, 1970], which is therefore presumed to be the real basis for the photoelectric data employed by MCNP4c2.

The photon data that are compatible with, and supplied with, MCNP4c2 are stored in the ACE* *mcplib* tables with the identifiers *.01p* and *.02p*. The latter is the default and is a superset of the former, featuring additional high energy (~MeV upwards) data. Photon data available to MCNP5 are those stored in the ACE *mcplib* tables referenced in the form: *.01p*, *.02p*, *.03p* and *.04p*. Table *.03p* is an extended version of *.02p*, expanded to include the momentum profile of the bound atomic electrons and the probabilities of interactions with electrons in particular shells [Biggs *et al*, 1975], allowing the energy of photons exiting incoherent collisions to be better sampled (Doppler broadening). Ultimately, therefore, tables *.01p* to *.03p* are all predominantly based upon the same original cross sections. Table *.04p* contains the updated EPDL97 library [Cullen *et al*,

* A Compact ENDF.

1997], as well as the bound-electron interaction / momenta data of [Biggs *et al*, 1975]. Table *.04p* is the MCNP5 default.

There are fewer data points available in Table *.02*p than in Table *.04p*; to illustrate, between 10 keV and 80 keV (inclusive) data are provided for nitrogen in Table *.02p* at eight discrete energies, whereas the same energy range in Table *.04p* contains forty seven such data points. However, differences in the number present for a given element are not simply a result of the *.04p* energy grid being uniformly finer than that of *.02p*, because the increase in the newer work can also sometimes be attributed to concentration around particular energies in order to resolve features such as photoelectric absorption edges. Nevertheless, the energy grids of Table *.02p* are generally coarse compared to Table *.04p*, and hence the relative lack of data in the former will have consequences for the accurate interpolation of values at any intermediate energies that are required. Both MCNP4c2 and MCNP5 effectively use a log-log interpolation between data points by default.

For the low Z materials of interest presently, [Storm & Israel, 1970] estimates a standard uncertainty of ~10 % in its photoionization data between ~5 keV and 200 keV. On the other hand, [Cullen *et al*, 1997] estimate a standard uncertainty in the EPDL97 library photoionization data of 2 % between 5 keV and 100 keV, and 1-2 % between 100 keV and 10 MeV.

The Table *.02p* and Table *.04p* data may be compared by ratio. Figure 3 gives the quantity $S_A(E) = [\sigma(E)_{A,(04)}] \div [\sigma(E)_{A,(02)}]$, where $\sigma(E)_{A,(X)}$ is the photon cross section at energy E for air according to Table *.Xp* data, calculated by taking the linear sums of the photoelectric, coherent and incoherent cross sections extracted directly from the tables for the individual elements, and applying an appropriate weighting scheme (i.e. assuming air comprises of 0.755268 N, 0.231781 O, 0.012827 Ar and 0.000124 C by mass-ratio [Hubbell & Seltzer, 1995]). The results shown in Figure 3 are at the eight common energies between 10 keV and 80 keV for which data are provided in Table *.02p* for N, O, C and Ar; where matching-energy data are not tabulated for a particular element in *.04p*, a logarithmic, 4-point, Lagrangian interpolation polynomial method is applied to it using the nearest two data points greater than, and two data points less than, the energy required. As is evident, the differences exhibited in $S_A(E)$ are significant, being for some energies a substantial fraction of the uncertainty [Storm & Israel, 1970] on $\sigma(E)_{A,(02)}$ and several standard deviations [Cullen *et al*, 1997] of the $\sigma(E)_{A,(04)}$ data.

Additionally shown in Figure 3 are the ratios, $H_A(E)$, of the heating numbers, $H_A(E) = [H(E)_{A,(04)}] \div [H(E)_{A,(02)}]$, where $H(E)_{A,(X)}$ is the average energy lost per collision in air by a photon of energy E, according to Table *.Xp* data. $H(E)_{A,(X)}$ is obtained from the raw heating data tabulated for each element by suitably weighting for air in the manner used to evaluate $S(E)_{A,(X)}$; the same energy grid between 10 keV and 80 keV is again adopted, with the same interpolation scheme used when necessary for the *.04p* data. Average heating numbers are utilized by MCNP *f6* tallies to estimate energy deposition per unit mass, analogously to the method employed elsewhere involving mass energy-transfer and mass energy-absorption coefficients, which are similarly dependent on photon average energy losses [Hubbell & Seltzer, 1995]. Specifically, for example, for a small test volume of matter surrounded by vacuum and exposed to a monoenergetic photon source, the absorbed dose per fluence assessed from the MCNP *f6:p* tally is approximately proportional to the product of the total cross section and the average heating per collision at that energy for that material. The ratios of the air kerma that might be expected from using Table *.04p* data, to those expected from using Table *.02p* data, may therefore be estimated at the above energies by multiplying $S_A(E)$ by $H_A(E)$; these products are also shown in Figure 3.

Note that changes in cross section data do not just affect the *f6* tallying process: the Monte Carlo simulation itself is also altered. Specifically, different cross sections can imply different outcomes to the interactions between photons and the atoms of the material, and hence the choice of data library influences the actual random walk of the individual particles as they are transported through a medium. Moreover, the effects of such deviations, however small, are likely to be amplified as the photon progresses through the geometry.

The changes in the available cross section data are not the only differences between MCNP4c2 and MCNP5. However, using MCNP5, but with the non-default Table *.02p* data, to repeat the calculations of $K(0,E)_{\text{air}}$ at selected energies where the MCNP5 / MCNP4c2 disparities are greatest, produces results that are irresolvable from those generated by MCNP4c2. This latter agreement further supports the conclusion that it is, indeed, the updating of the cross section libraries, and not any other changes to the way in which photons are transported or tallied, that has led to the discrepancies shown in Figures 1 and 2.

Summarizing, *.02p* and *.04p* data are different in a way that is significant given their standard uncertainties, and so their uses can lead to results that disagree. The magnitude of these differences are highlighted for air in Figure 3, but changes in the cross sections and heating data for the various other materials involved in the TLD calculations, such as ^{7}LiF:Mg,Cu,P, PTFE or PP, are also likely to contribute to the disparities between the MCNP4c2 and MCNP5 relative response results.

As a final remark, note that although the changes in cross section data lead to sizeable discrepancies in the dosemeter response results, their effect could be even greater for situations that involve significant attenuation. For example, it might be expected that the results obtained by MCNP5 (using *.04p* tables), for a shielding calculation featuring photons in the 10-100 keV energy range, could imply that less shielding material is required than when the same calculation is performed using MCNP4c2. This could have serious consequences, though, fortunately here, it is the newer data that would lead to the less conservative estimate.

4.2 Mass Attenuation / Energy Absorption Coefficients

Removing the renormalization of the [Scofield, 1973] data, as advocated by [Saloman *et* al, 1988] and used in [Hubbell & Seltzer, 1995] and MCNP5, is thought to change the cross sections by up to a few percent, compared to the renormalized scheme used in [Hubbell, 1982]. For a stated coefficient, and for a material and energy range of interest, the differences between the [Hubbell & Seltzer, 1995] values and those of [Hubbell, 1982] may be illustrated by plotting the ratio, *M('95/'82)*, defined by Equation (2), where the data used are either the mass attenuation coefficients, (μ/ρ), or the mass-energy absorption coefficients, (μ_{en}/ρ), as required. Recall that for a given element, (μ/ρ) is directly proportional to its photon total cross section. The ratios, *M('95/'82)*, for air from 1 keV to 1 MeV are shown in Figure 4. It should, however, be noted that uncertainties in the [Hubbell, 1982] mass attenuation coefficients are estimated by Hubbell to be approximately $\pm$ 5 % at energies below 5 keV and up to $\pm$ 2 % for the remainder, with uncertainties for (μ_{en}/ρ) thought to be slightly greater. These uncertainties are subjective judgements that reflect: "…*differences of measured values among independent experimenters, and the magnitudes of* ad hoc *adjustments, corrections and extrapolations of quantities entering into the computation of cross sections from incomplete available theory*" [Hubbell, 1982]. Uncertainties in the [Hubbell & Seltzer, 1995] data do not appear to be provided in the document.

$$M('95/'82) = \frac{(Hubbell \,\&\, Seltzer \text{ '95 } data)}{(Hubbell \text{ '82 } data)} \qquad (2)$$

From Figure 4, it is evident that increases of up to around 2 % are found in both the mass attenuation and the mass-energy absorption coefficients when comparing [Hubbell & Seltzer, 1995] to [Hubbell, 1982] values, with maximum differences occurring at ~10 keV and ~15 keV respectively. These increases are approximately equal to one standard deviation uncertainty of the [Hubbell, 1982] data. Although such a difference is not significant, it may still be considered large given that it results only from the un-renormalizing of the [Scofield, 1973] data.

4.3 Conversion Coefficients

As a last aside, note that the air kerma to personal dose equivalent conversion coefficients for monoenergetic photons featured in [ICRU, 1998] and [ICRP, 1996] for $H_p(10)$ and $H_p(0.07)$, and hence the interpolated values given by ISO 4037-3 [ISO, 1999] and [Ankerhold, 2000] for the Narrow Series fields, are based on data from [Grosswendt *et al*, (unp.)] that are unpublished. Specifically, Paragraph 195 of [ICRU, 1998] / [ICRP, 1996] describes:

> "*ICRU Report 47 has recommended conversion coefficients for $H_{p,slab}$ in the ICRU slab based on calculations by [Grosswendt, 1990]. Data from [Till et al,1995] and revised data from [Grosswendt et al, (unp.)] were used in the preparation of Tables A.24 and A.25 of Annex 2, which also contain conversion coefficients from air kerma as well as angular-dependence factors for $H_p(10,\alpha)$ and $H_p(0.07,\alpha)$ for angles between 0° and 75°.*"

Data from [Hubbell *et al*, 1975], [Hubbell, 1977], [Hubbell & Øverbø, 1979] and [Hubbell, 1982] are used in [Grosswendt, 1990]; exactly how the work is revised for the unpublished [Grosswendt *et al*, (unp.)] is not clear. The actual sources of the cross section data (or, indeed, the method even) used in the determination of the conversion coefficients presented in [ICRU, 1998] / [ICRP, 1996] are not readily ascertained, therefore.

However, two sets of air kerma per fluence conversion coefficients are presented in [ICRU, 1998] / [ICRP, 1996] for monoenergetic photons. One of these was derived from [Hubbell, 1982] data; the other was compiled using the newer [Hubbell & Seltzer, 1995] data.

Fluence to personal dose equivalent conversion coefficients do not appear to be available in the discussed literature, either for monoenergetic photon fields [ICRU, 1998; ICRP, 1996] or the Narrow Series distributions [Ankerhold, 2000; ISO, 1999]. These could be calculated indirectly from the air kerma to personal dose equivalent and air kerma per fluence conversion coefficients, but the lack of clarity regarding the cross section data used for the former would, of course, then be transferred.

5 SUMMARY, DISCUSSION AND CONCLUSIONS

The above analyses raise two issues that will have to be addressed when further calculations involving the TLD are considered in the future. Firstly, given that fluence to personal dose equivalent conversion coefficients are not readily available in their own right, and that the source of the cross section data used by [Grosswendt *et al*, (unp.)] to determine the air kerma to personal dose equivalent conversion coefficients is not clear, what is the best reference for obtaining $h(\theta,E)$ for Equation (1), in order to avoid potential systematic uncertainties? Putting this issue another way: how compatible might the MCNP5 table *.04p* cross sections be with whatever data were utilized by Grosswendt? Of course, one solution here might be to use MCNP5 to generate a new set of conversion coefficients; but, given the ‘official’ status of the [ICRU, 1998] / [ICRP, 1996] data, could such results then be used in any serious capacity?

Secondly, given that the efficiency function, $\eta'(E)$, featured in Equation (1) was derived using MCNP4c2 [Eakins *et al*, 2007], and hence the default *.02p* cross section library, how appropriate is its use in any calculation performed by MCNP5 with its newer default data? For example, despite MCNP5 having access to superior cross section libraries (*.04p* and *.03p*), might potential incompatibility with the efficiency function imply that it would still be better to instead use the older tables in the future, or even the older MCNP4c2 code itself, and hope that any systematic uncertainties contained in $\eta'(E)$ are to some extent cancelled out? Or, must a new, MCNP5-derived efficiency function be determined? It is not clear at this stage what the preferred options would be to address either of these two issues, though in an ideal situation the efficiency parameter would be evaluated experimentally.

It is evident from Figure 2 that updating from MCNP4c2 to MCNP5 changes the response characteristics that are calculated for the new HPA TLD, with Figure 1 showing the changes in absorbed dose calculated in both the TLD elements and in air. The largest differences in each case arise at low energies (< 100 keV) and can be as great as around 10 %. Moreover, it is evident from Figures 3 and 4 that the most likely origin of this discrepancy is the upgrading of the photon cross section and heating data that are used by default. Indeed, when the products of the cross section and heating data taken from either the *.02p* or the *.04p* libraries are compared for air, as featured in

Figure 3, low-energy differences are exhibited that are as large as those seen in Figure 1. Changes in the data tabulated for the various other materials of importance to the TLD will also contribute to the disagreements between the MCNP4c2 and MCNP5 relative response results. It is quite possible, then, that had MCNP5 been available to HPA during the TLD design project, the final, optimized specifications of the device might have been subtly different, though it is emphasized that experimental validation and extensive type-testing of the new dosemeter have demonstrated satisfactory performance [Gilvin *et al*, 2007; Eakins *et al*, 2007], and that the response changes of up to ~10 % attributed to the changes in the cross section data nevertheless still leave the overall accuracy of the dosemeter, at the 95 % confidence level, within the uncertainty factor [ICRP, 1997] of 1.5 typically tolerated in radiation protection.

As always, therefore, the general reminder from this work is consequently that Monte Carlo techniques can provide a useful tool for applications in radiological safety, but should not be assumed to produce an exact answer and are not a complete substitute for measurements. In short, a Monte Carlo code or an analytical approach can only ever be as good as the data upon which it relies, and the inherent uncertainties, inaccuracies, limitations and inadequacies in these should never be ignored by the user.

6 ACKNOWLEDGEMENTS

The author would like to thank Ulrike Ankerhold of Physikalisch-Technische Bundesanstalt (PTB) for supplying data on the Narrow Series photon distributions. Special thanks also to Jan Jansen and Rick Tanner, of HPA, and David Bartlett, formerly of HPA, for comments and advice.

7 REFERENCES

Eakins JS, Bartlett DT, Hager LG, Molinos-Solsona C. and Tanner RJ (2007). The MCNP-4c2 design of a two element photon / electron dosemeter that uses magnesium / copper / phosphorus doped lithium fluoride. *Radiat. Prot. Dosim*., **128**, 12-20.

Gilvin PJ, Baker ST, Daniels TJ, Eakins JS, McClure DR, Bartlett DT and Boucher C (2007). Type testing of a new TLD for the UK Health Protection Agency. *Radiat. Prot. Dosim*., **128**, 21-35.

Briesmeister JF (Ed.) (2000). MCNP - A general Monte Carlo N-particle transport code, Version 4C. Los Alamos National Laboratory, Report LA-13709-M.

X-5 Monte Carlo Team (2003). MCNP - A general Monte Carlo N-Particle transport code, Version 5. Los Alamos National Laboratory, Report LA-UR-03-1987.

Ankerhold U (2000). Catalogue of X-ray spectra and their characteristic data - ISO and DIN radiation qualities, therapy and diagnostic radiation qualities, unfiltered X-ray spectra. PTB-Dos-34 (Braunschweig:PTB).

International Organization for Standardization (ISO) (1996). X and gamma reference radiation for calibrating dosemeters and doserate meters and for determining their response as a function of photon energy - Part 1: Radiation characteristics and production methods. ISO 4037-1, (Geneva:ISO).

International Organization for Standardization (1999). X and gamma reference radiation for calibrating dosemeters and doserate meters and for determining their response as a function of photon energy - Part 3: Calibration of area and personal dosemeters and the measurement of their response as a function of energy and angle of incidence. ISO 4037-3, (Geneva:ISO).

Hubbell JH, Veigele WJ, Briggs EA, Brown RT, Cromer DT and Howerton RJ (1975). Atomic form factors, incoherent scattering functions, and photon scattering cross sections. *J. Phys. Chem. Ref. Data*, **4**, 471.

Everett CJ and Cashwell ED (1973). MCP code fluorescence routine revision. Los Alamos Scientific Laboratory report LA-5240-MS.

Hubbell JH (1982). Photon mass attenuation and energy-absorption coefficients from 1 keV to 20 MeV. *Int. J. Appl. Radiat. Isot*. **33**, 1269-1290.

Hubbell JH, Veigele WJ, Briggs EA, Brown RT, Cromer DT and Howerton RJ (1977). Atomic form factors, incoherent scattering functions, and photon scattering cross sections. (Erratum). *J. Phys. Chem. Ref. Data*, **6**, 615-6.

Hubbell JH and Øverbø I (1979). Relativistic atom form factors and photon coherent scattering cross sections. *J. Phys. Chem. Ref. Data*, **8**, 69.

Scofield JH (1973). Theoretical photoionization cross sections from 1 to 1500 keV. Lawrence Livermore Laboratory, Report UCRL-51326.

Hubbell JH and Seltzer SM (1995). Tables of X-ray mass attenuation coefficients and mass energy-absorption coefficients 1 keV to 20 MeV for elements Z = 1 to 92 and 48 additional substances of dosimetric interest. National Institute of Standards and Technology, NISTIR 5632.

Saloman EB, Hubbell JH and Scofield JH (1988). X-Ray attenuation cross sections for energies 100 eV to 100 keV and elements Z=1 to Z=92. *At. Data Nucl. Data Tables*, **38**, 1-197.

Cullen DE, Hubbell JH and Kissel LD (1997). EPDL97: The evaluated photon data library, ‘97 version. Lawrence Livermore National Laboratory, UCRL-50400, Vol. 6, Rev. 5.

Hubbell JH (1997). Summary of existing information on the incoherent scattering of photons particularly on the validity of the use of the incoherent scattering function. *Radiat. Phys. Chem*., **50(1)**, 113-124.

Cullen DE (1989). Program SCATMAN: A code designed to calculate photon coherent scattering anomalous scattering factors and cross sections. Lawrence Livermore National Laboratory, UCRL-ID-103422.

Halbleib JA, Kensek RP, Mehlhorn TA, Valdez GD, Seltzer SM and Berger MJ (1992). ITS Version 3.0: Integrated TIGER series of coupled electron/photon Monte Carlo transport codes. SAND91-1634.

Cashwell ED, Neergaard JR, Everett CJ, Schrandt RG, Taylor WM and Turner GD (1973). Monte Carlo photon codes: MCG and MCP. Los Alamos Scientific Laboratory, Report LA-5157-MS.

Storm E and Israel HI (1970). Photon cross sections from 1 keV to 100 MeV for elements Z=1 to Z=100. *Nuclear Data Tables*, **7**, 565. See also: Israel HI and Storm E (1967). Photon cross sections from 0.001 to 100 MeV for elements 1 through 100. Los Alamos Scientific Laboratory, Report LA-3753.

Biggs F, Mendelsohn LB and Mann JB (1975). Hartree-Fock Compton profiles for the elements. *Atomic Data and Nuclear Data Tables*, **16(3)**, 201-309.

International Commission on Radiation Units and Measurements (ICRU) (1998). Conversion coefficients for use in radiological protection against external radiation. Report 57.

International Commission on Radiological Protection (ICRP) (1996). Conversion coefficients for use in radiological protection against external radiation. Publication 74.

Grosswendt B, Buermann L, Kramer HM, Till E and Zankl M (Unpublished). Reference coefficients $H_p(0.07,\alpha)$ and $H_p(10,\alpha)$ from air kerma to the dose equivalent quantities in the ICRU slab.

Grosswendt B (1990). Conversion coefficients for calibrating individual photon dosimeters in terms of dose equivalents defined in an ICRU tissue cube and PMMA slabs. *Radiat. Prot. Dosim.*, **32**, 219-231.

Till E, Zankl M and Drexler G (1995). Angular dependence of depth doses in a tissue slab irradiated with monoenergetic photons. Gesellschaft fűr Strahlen und Umweltforschung mbH, Germany, GFS-Bericht 27/95.

Hubbell JH (1977). Photon mass attenuation and mass energy-absorption coefficients for H, C, N, O, Ar, and seven mixtures from 0.1 keV to 20 MeV. *Radiat. Res*. **70**, 58.

International Commission on Radiological Protection (1997). General principles for the radiation protection of workers. Publication 75.

8 FIGURES

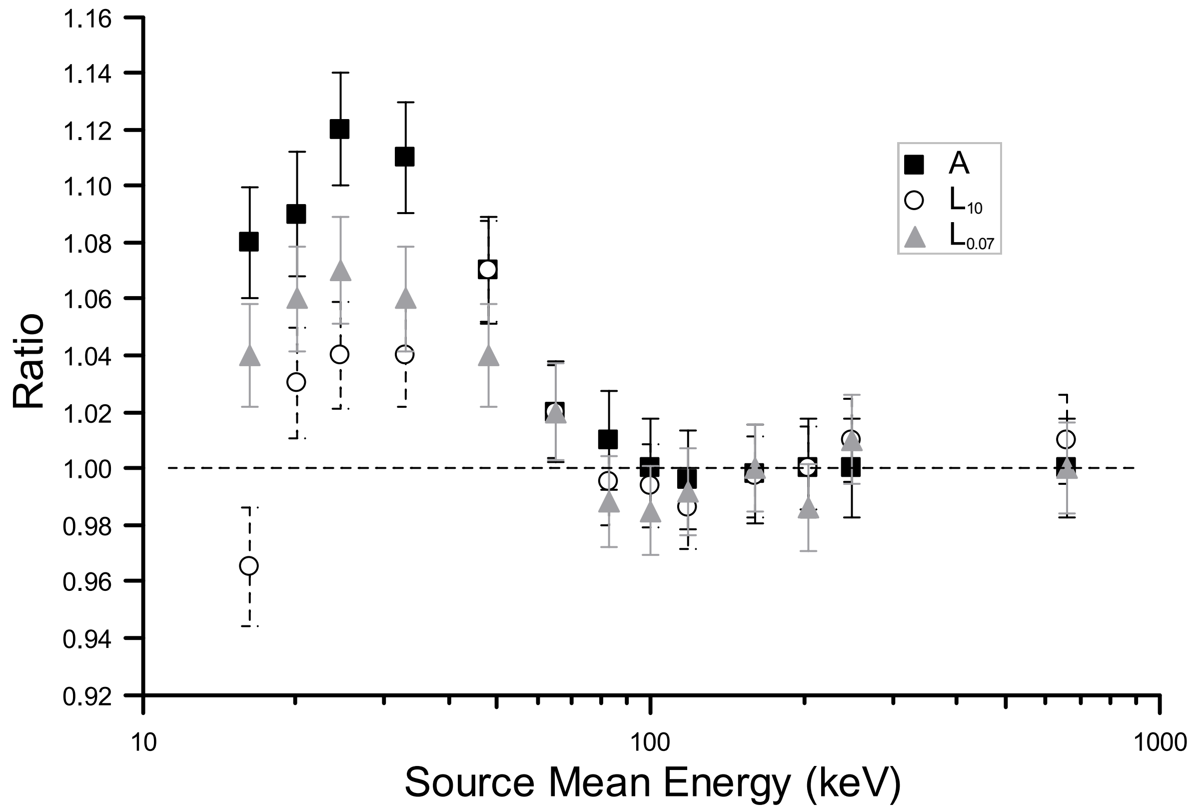

Figure 1: The ratios A = [$K(0,E)_{air,(5)}$]÷[$K(0,E)_{air,(4c2)}$], L_{10} = [$K(0,E)_{LiF,(5)}$]÷[$K(0,E)_{LiF,(4c2)}$] and $L_{0.07}$ = [$K(0,E)_{LiF,(5)}$]÷[$K(0,E)_{LiF,(4c2)}$] between 10 keV and 1000 keV, where $K(0,E)_{M,(5)}$ is the absorbed dose in material M calculated using MCNP5 for a photon source of mean energy E, $K(0,E)_{M,(4c2)}$ is the absorbed dose in material M for a photon source of mean energy E calculated by MCNP4c2, and the subscripts '10' or '0.07' on L indicate whether it is the $H_p(10)$ or the $H_p(0.07)$ element that is being tallied. Error bars indicate one standard deviation uncertainty.

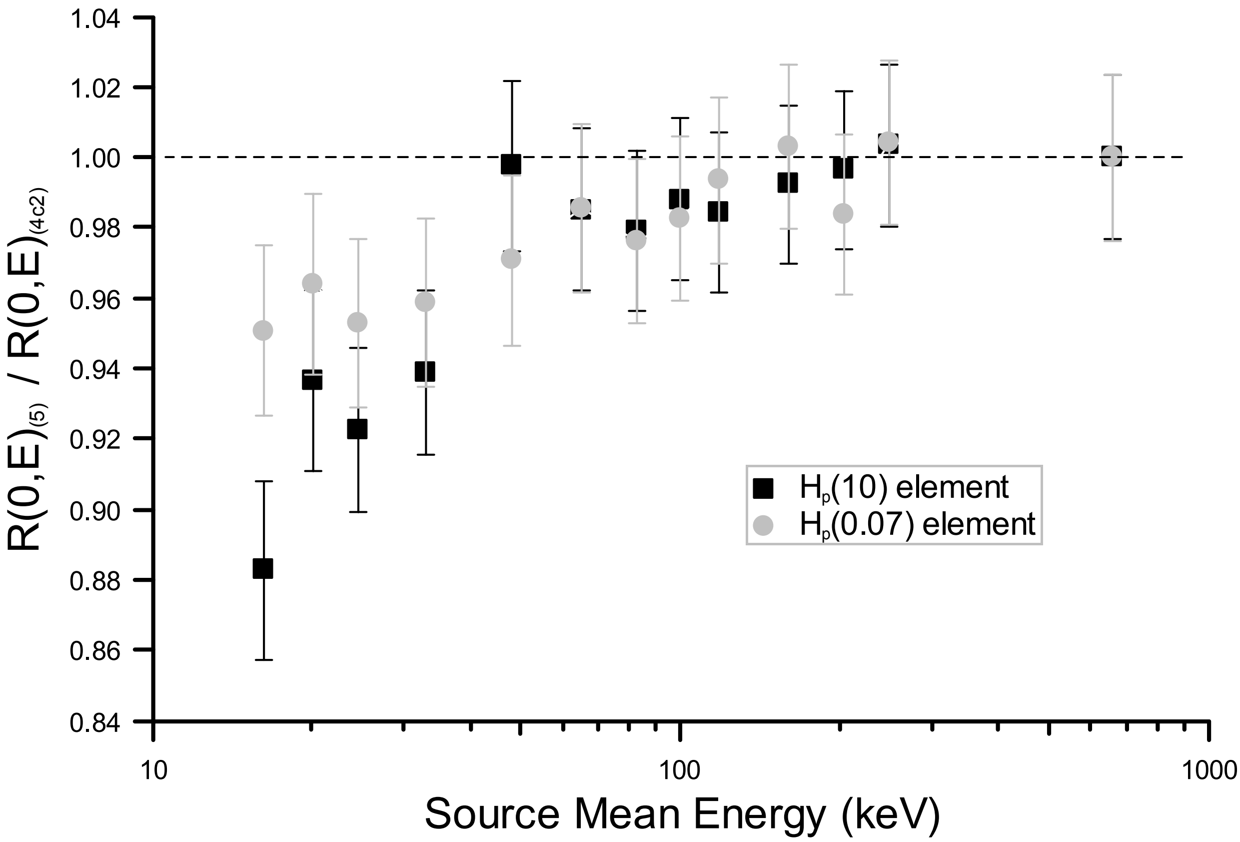

Figure 2: **The ratios [$R(0,E)_{(5)}$]÷[$R(0,E)_{(4c2)}$] between 10 keV and 1000 keV, where $R(0,E)_{(5)}$ is the relative response of the TLD calculated using MCNP5 for a photon source of mean energy E incident normally, and $R(0,E)_{(4c2)}$ is the analogous relative response calculated by MCNP4c2. The ratios for both the $H_p(10)$ and the $H_p(0.07)$ elements are shown. Error bars indicate one standard deviation uncertainty.**

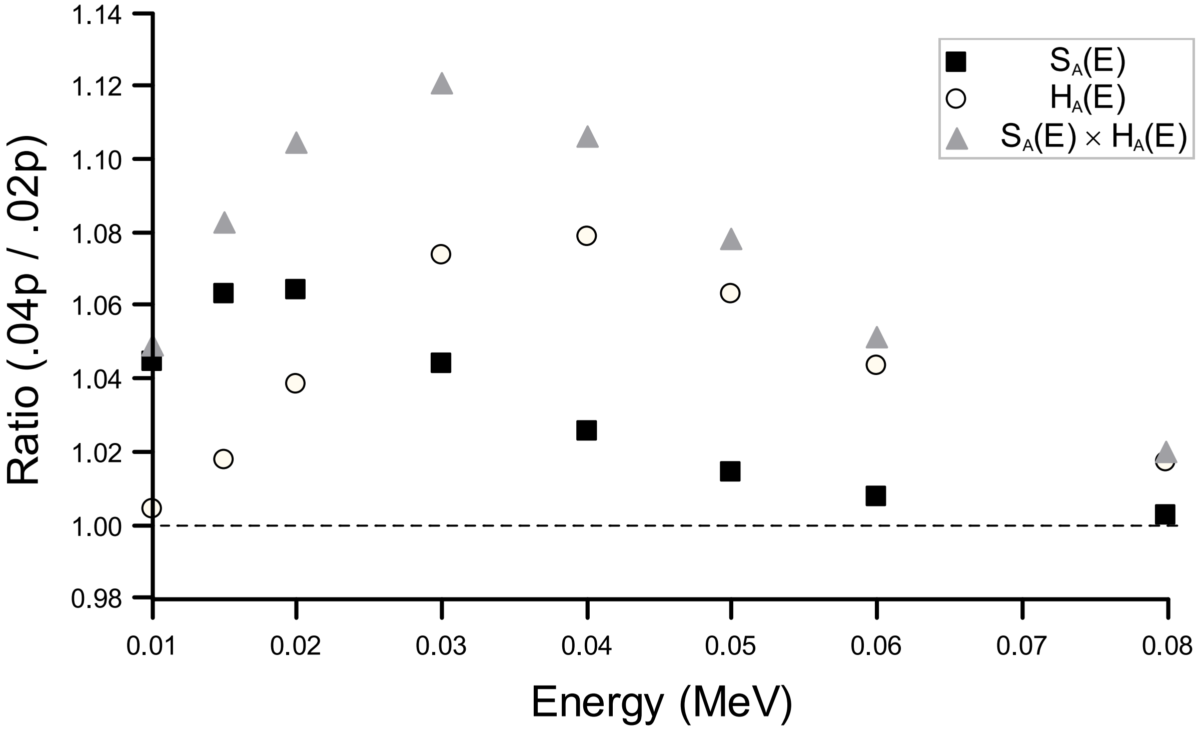

Figure 3: **The ratios of Table *.04p* to Table *.02p* photon cross section data [$S_A(E)$], and average heating per collision data [$H_A(E)$], for air between 10 keV and 80 keV. The product $S_A(E) \times H_A(E)$ is also shown.**

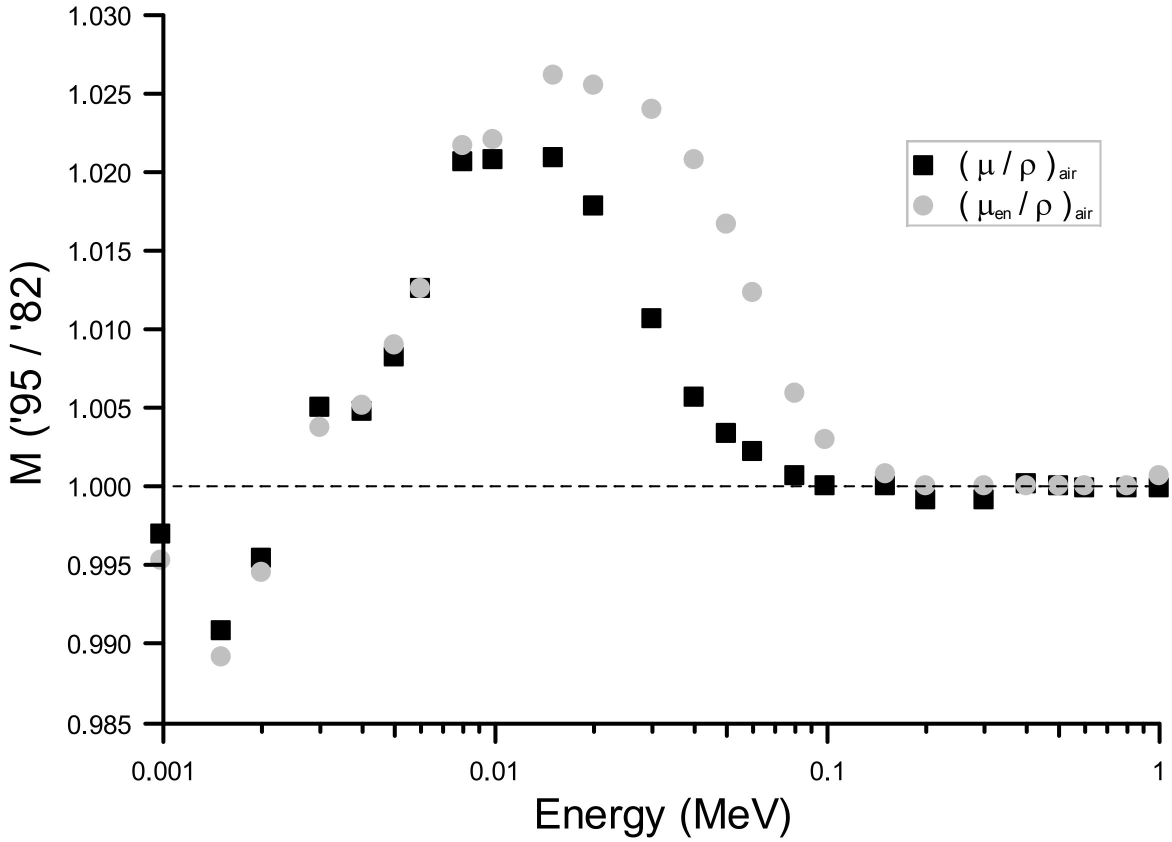

Figure 4: The ratios, for air, of [Hubbell & Seltzer, 1995] to [Hubbell, 1982] mass attenuation coefficients (μ/ρ), and of [Hubbell & Seltzer, 1995] to [Hubbell, 1982] mass-energy absorption coefficients (μ_{en}/ρ).